

# Detection of Dementia and Classification of its Stage Using Image Processing

Shraman Jain<sup>1</sup>, Abhishek Gudipalli<sup>2\*</sup>, Shrey Jain<sup>3</sup>

Submitted: 05/02/2024 Revised: 13/03/2024 Accepted: 19/03/2024

**Abstract:** Humans are increasingly being diagnosed with dementia, a disease that can seriously impair their quality of life. With the development of cutting-edge medical technology, it is crucial to precisely detect and identify dementia as soon as possible so that necessary action may be performed. The purpose of the manuscript is to present a precise approach for determining dementia and its stage from MRI images. This is accomplished by combining pre- and post-image processing methods with the watershed segmentation and threshold algorithms. The suggested method not only locates the affected region but also improves image quality using noise removal methods. When validated with a variety of evaluation criteria, including as Peak Signal-to-Noise Ratio (PSNR) Structural Similarity Index Measure (SSIM), Entropy Feature Similarity Index Measure (FSIM), Normalize Cross Correlation (NCC), Normalized Absolute Error (NAE) and stand out when compared to other comparable existing algorithms.

**Keywords:** Dementia, Stages, MRI, Evaluation parameters, Watershed segmentation, MSER

## 1. Introduction

Around 55 million individuals worldwide have dementia, and more than 60% of them reside in low- and middle-income nations. This number is anticipated to increase to 78 million in 2030 and 139 million in 2050 due to the fact that the proportion of older people in the population is rising in almost every country. The term "dementia" is used to describe a collection of symptoms that significantly impair memory, reasoning, and social functioning. Dementia isn't caused by one specific illness, but by a number of illnesses. Dementia comes in a variety of forms. The most prevalent type, which may account for 60–70% of cases, is Alzheimer's disease. Other significant forms of dementia include vascular dementia, dementia with Lewy bodies (abnormal protein clumps that occur inside nerve cells), and a number of illnesses that exacerbate frontotemporal dementia (degeneration of the frontal lobe of the brain). Apart from this, it can also be categorized in stages namely very mild, mild, and moderate.

Even though memory loss is a common symptom of dementia, it might have various underlying causes. And although memory loss is frequently one of the first symptoms of dementia, it does not

necessarily signify that you have the disease. The most frequent cause of a progressive dementia in older persons is Alzheimer's disease, although there are several other dementia-related conditions as well. Some symptoms of dementia may be treatable, depending on the underlying cause. Damage to or loss of brain's nerve cells and connections is what leads to dementia. Dementia can have varied effects on different people and produce distinct symptoms depending on the part of the brain that is affected. Dementias are frequently categorised according to characteristics they share, such as the protein or proteins deposited in the brain or the area of the brain affected. Some illnesses that resemble dementias, particularly those brought on by pharmaceutical interactions or vitamin shortages, may get better with treatment. There is no cure for dementia, however early diagnosis promote early and optimal management. People may take charge of their disease, make plans for the future, and live well with dementia with the aid of an early diagnosis and access to the necessary services and support. By doing so, the likelihood that memory, communication, behaviour, or other issues are caused by other, potentially treatable illnesses with dementia-like symptoms will be reduced. Making the most of their talents, having access to helpful resources and support, and maybe benefiting from available medical and non-medical treatments can all aid people with dementia. Someone who

<sup>1,2</sup>School of Electrical Engineering, Vellore Institute of Technology, Vellore, 632014, Tamil Nadu, India.

<sup>3</sup>Department of Biotechnology, Thapar Institute of Engineering and Technology, Patiala, 147004, Punjab, India.

\* Corresponding Author Email: abhishek.g@vit.ac.in

receives an early diagnosis has the opportunity to discuss the changes taking place in their life with family and friends. A person with dementia may have the chance to assess their financial status and talk with family members or legal professionals about making plans for a long-term power of attorney or an advance decision. There is compelling evidence that someone with dementia can live longer in their own home and remain independent with an early diagnosis. This improves the quality of life for those with dementia and their carers and results in significant savings on long-term care expenditures by preventing early or needless admission to a care facility or hospital. The earlier someone is diagnosed, the more successful pharmacological and non-drug treatments can be.

There are many applications of image processing, medical industry being one of them. Medical image processing encompasses the use and exploration of image datasets of the human body, obtained most commonly from a Computed Tomography (CT) or Magnetic Resonance Imaging (MRI) scanner to diagnose pathologies or guide medical interventions such as surgical planning, or for research purposes. Medical image processing is carried out by radiologists, engineers, and clinicians to better understand the anatomy of either individual patients or population groups. Medical image processing's key advantage is that it enables thorough, non-invasive investigation of internal anatomy. In recent years, it has emerged as one of the most important instruments used to enhance medicine. Accurate digital reproduction of anatomical structures at various scales and with widely varied properties, such as bone and soft tissues, is made possible by the ever rising image quality in combination with cutting-edge software tools. A more thorough understanding is possible, for instance, of interactions between patient anatomy and medical devices, thanks to measurement, statistical analysis, and the development of simulation models that take real anatomical geometries into account.

A common way to diagnose dementia is via MRIs. However, they are manually read. They also require time and manual labor. A system that can accurately identify the dementia-affected area, categorise its stage, and improve current testing processes is required. It must also be labour- and money-efficient while maintaining the patient's health. In the field of brain disorders, image

processing has become the front-runner. Compared to the currently in use systems, it has produced results that are more accurate. It might be successfully incorporated into common clinical practice with a wider area of extension. In order to automate dementia detection, this project aims to create a tool for dementia detection and classification of its stage. The goal is to develop an algorithm based on watershed algorithm and threshold segmentation that can accurately and precisely diagnose dementia with the least amount of manual involvement by detecting dementia in an MRI scan and classifying its stage using MSER. The article discusses the application of the numerous operations that make up the suggested algorithm as well as the subsequent analysis of the results.

MRI scans are accepted as input by the suggested algorithm. The gray-scale image is given a median filter to remove noise. A smoothing matrix in the form of an average filter is then used to smooth the image. After smoothing, the top hat filter is applied to the image to eliminate noise from the foreground. After that, contrast enhancement is applied in order to saturate the pixel intensity. The improved image is then subjected to image binarization before going through morphological erosion to get rid of any extra pixels from the MRI image's borders. Morphological dilation increases the quality of the image by adding pixels to fill in any gaps and holes that may have been created by the presence of noise within the image borders. Now the threshold algorithm is carried out. The average intensity value of each pixel in the image is used to compute and establish the threshold value in this. Watershed segmentation is done using the obtained image. Watershed segmentation is followed by K-means clustering and MSER detection. The final output includes a highlight of the dementia-detected region. By counting the MSER and referring to the table provided (table 1), we can know the stage of dementia. Last but not least, the proposed method's performance is assessed using a number of parameters, including the Peak Signal-to-Noise Ratio (PSNR), Structural Similarity Index Measure (SSIM), Entropy, the Feature Similarity Index Measure (FSIM), Normalize Cross Correlation (NCC), and the Normalized Absolute Error (NAE). The results give a glimpse into

how well the aforementioned methods can improve image quality.

The method mentioned doesn't need a lot of computing power or training data. Deep learning is unnecessary because traditional image processing frequently uses less lines of code and can handle a problem more effectively than deep learning. The training dataset, if badly designed, will probably perform poorly for images other than the training set since the features learnt from a deep neural network are particular to the training dataset. Large datasets can help with these issues, but closed applications cannot support the enormous amount of research required. Take the issue of product categorisation as an illustration. Assume that the challenge is to categorise food cans on a conveyor belt as vegetarian or non-vegetarian based on their colour — green for vegetarian, red for non-vegetarian. In this case, traditional image processing is favoured due to its straightforward colour thresholding technique, even if accurate DL models can be produced by gathering sufficient training data.

The suggested approach is also compared with two other existing algorithms, which differ mainly in the pre- and post-processing methods used, in order to verify the results achieved. This comparison sheds light on the significance of selecting the right pre- and post-processing methods and their influence on the results.

Image processing when used with Convolutional Neural Networks (CNN) or Machine Learning (ML) algorithms like regularized General Linear Model regression (GLMs), Support Vector Machines (SVMs) with a radial basis function kernel, and single-layer Artificial Neural Networks can also be equipped to train data. In this methodology, the output is based on extensive noise removal and real-time execution of functions. When paired with neural network or machine learning, the program can be trained with various inputs to reduce errors. This training can also ensure the reduction of human intervention in calculation.

## 2. Literature Survey

The literature review is broken down into themes such as areas that use image processing, applications in the medical field, techniques that are similar across applications, and finally, new machine learning and deep learning techniques, which highlight the gaps in our knowledge while

also motivating us to incorporate them into our algorithm in the future.

For civil engineers, the lifespan and quality of the pavement services are crucial since they have a direct impact on the users' access to regular services. Therefore, it is essential to keep track of the condition of the pavement before irreparable damage occurs in order to schedule maintenance in a timely manner, which in turn ensures the safety of public transit. By keeping an eye on the structure's dynamic responses and assessing the state of the road's surface, numerous pavement defects can be identified and studied. Advanced technologies, such as different invasive sensing techniques, image processing techniques, and machine learning approaches, can be used for the collecting and analysis of such data. Hou, Yue, et al(2021) highlights the most recent state-of-the-art in intrusive sensing, image processing, and machine learning methods for pavement monitoring and analysis and makes suggestions for future advances in these areas. Throughout its service life, a pavement's structural integrity is impacted by heavy traffic loads and harsh environmental conditions. The performance of intrusive sensors must be enhanced, and their packaging must be optimised to fulfil the demands of low power consumption, low cost, high precision, high integration, compression resistance, and waterproofing. Many of the current image processing methods are unable to automatically adapt to every form of pavement image because pavement field photos have a wide range of properties. Therefore, more study is required to enhance the algorithm's ability to adapt to include images with a variety of diverse situations. To collect a significantly larger dataset, further field and laboratory testing on the capabilities and conditions of pavement are required. The detection and identification of additional pavement distresses using machine learning techniques is also necessary.

Consistent crack and other structural anomaly inspections are necessary for gas turbine maintenance. The inspections produce information for assessing structural health and repair costs as well as information on the general state of the structures. Automated visual crack identification has been attempted in the past using a variety of image processing approaches, with varied degrees of success. Mohtasham Khani, Mahtab, et al (2020) proposes a novel framework for fracture

detection that combines methods from deep learning and traditional image processing. This work's key contribution is the proof that pre-processing image data with filters can greatly improve the classification performance of a convolutional neural network-based model. During the detection phase, a CNN trained on 700 annotated and pre-processed gas turbine images was used. On a set of cracked surface images gathered from gas turbines, the built architecture surpasses comparable efforts by producing a classification accuracy of 96.26%.

Wang, Aichen, et al(2019) explains how machine vision mixed with image processing techniques has developed into a potential tool for accurate real-time weed and crop detection in the field, providing useful sensing information for site-specific weed management. The development of weed detection utilizing ground-based machine vision and image processing methods was discussed in this paper. The four methods for weed detection, specifically pre-processing, segmentation, feature extraction, and classification, were given in depth. Different colour indices and classification techniques, such as colour index-based, threshold-based, and learning-based ones, were developed to distinguish vegetation from background. The challenge in weed detection is separating crops from weeds, which may have identical characteristics. Weed identification applications based on traditional machine learning as well as recently developed deep learning-based algorithms were also presented. The difficulties and solutions for weed detection in the field, including leaf occlusion and overlap, variable lighting conditions, and various development stages, were also highlighted.

Nowadays, melanoma skin cancer is very problematic for health. Dermatologists' response times are sped up, and diagnosis accuracy is improved, when melanoma skin cancer is found early. It is necessary to have an automated computerised system for diagnosing skin cancer in its early stages due to the skin cancer epidemic's rapid rise. There are visual similarities across many of the skin cancer photographs. The process of removing characteristics from skin cancer photographs is a crucial and difficult undertaking. The dermatologists' ability to diagnose skin conditions and provide patients with better care is aided by the automated computerised diagnosis mechanism, which also helps to

increase the accuracy of analysis of skin disorders more quickly. Sreedhar, B., Manjunath Swamy BE, et al (2020) compares various image processing methods for skin cancer image classification, pre-processing methods, feature extraction, and image segmentation datasets using conventional image processing methods and current technology. Pre-processing an image is done to get rid of extraneous artefacts like noise, air bubbles, and fine hair. Several filtering methods, including median and Gaussian Filtering, can be used to remove skin hair. Enhance filtering can form out image borders and increase the precision of image segmentation in addition to contrast. Enhancing the form and size of an image is known as post-processing. To achieve image post-processing, Karhunen-Loève (KL) changes histogram equalisation and utilises several types of filters. The classification is done using Artificial Intelligence, Machine Learning, and Deep Learning based classification algorithm.

R.Anitha , Mr.Prakash, S.Jyothi(2016) uses segmentation technique for the medical images. Low brain activity and poor blood flow are the primary causes of Alzheimer's disease. The hippocampus region of the brain is a crucial part. Human behaviour is typically determined by the hippocampus function. It takes an expert many hours to manually segment the hippocampus. There are numerous segmentation techniques accessible in image processing. In this paper, the hippocampus region is segmented using a modified method based on the watershed algorithm. Two methods were used to convert the binary form of the brain images. Block mean, mask, and labelling concepts are used in the first method, and top hat, mask, and labelling concepts are used in the second. However, it is discovered that a portion of the image has holes in it, preventing proper segmentation. Image hole filling techniques are used to solve this issue, and similar components are gathered into connected components. Alzheimer's disease will be categorised as a result of the hippocampus' shape analysis.

According to Tarhini and Shbib (2020), MRI scans are preferable to CT scans for tumor diagnosis because they may produce a considerably more detailed image of the body part and are more suited to catching small or difficult-to-detect cancers. There has been a great deal of research

into how to combine diverse technologies to build automated systems that can quickly and correctly detect brain tumors. To emphasize the tumor location, their suggested technique first performs threshold segmentation and then watershed segmentation. Then, as part of the post-processing, morphological operators are utilized to improve the image quality. These systems are built using a variety of methods, including machine learning, deep learning, image processing and convolutional neural networks.

Professor Nisha V. M. and Shrikant Patro's 2019 research aims to identify Alzheimer's disease as early as possible so that patients can be treated before irreversible changes to the brain take place. They suggest an image processing method to process brain MRI data from the axial plane, coronal plane, and sagittal plane. In brain MRI, the affected region is highlighted via image segmentation. In a brain MRI, the hippocampus and total brain volume are the regions that are diagnosed. Alzheimer's disease patients, members of the healthy cohort, and people with mild cognitive impairment are identified in comparison. Mustaqem et al.(2012) pre-processes the image using median filter in combination with a Gaussian high pass filter to sharpen the image in order to find the detected tumor region. To highlight the tumor zone, they next perform threshold segmentation and watershed segmentation. A final image with a marked tumor location is produced using post-processing techniques that employ morphological processes including erosion and dilatation.

Shahin (2018) suggests a quick algorithm to find the tumor location. To obtain the gradient of the input image, sobel detector pre-processing is utilized. The skull area is then removed from the image using the skull-stripping process. The image is then subjected to watershed segmentation. In order to investigate and analyze the segmented area, the paper divides the characteristics of segmented areas into three categories: geometric, texture, and gradient. The Top-hat filter is the final post-processing technique used to lessen the brightness of the image.

Md. Abdullah Al Mahmud, AHM Zaidul Karim, Md. Sazal Miah, Yeong-gwang Kim, Jinsul Kim, and Shikder Shafiul Bashar (2020) use the patient's MRI imaging for the detection of spine tumors utilizing image processing for precisely identifying tumors. A typical method is

magnetic resonance imaging (MRI). It is a non-invasive method for creating topographic 3-dimensional images of the human body. For the detection of numerous anomalies in soft tissues, such as the spine, lesions, and tumors, MRI is widely used. The most challenging and developing field nowadays is clinical image processing. The essential concepts of image processing—segmentation, morphological operations, and various noise reduction functions—are all included in this method. MRI images will be used as input in their suggested technique. For the purpose of eliminating additional data, the input image will be converted to a grayscale image and then modified based on the maximum intensity level. Images of the spine's cross-section will be converted to binary data to determine its range. Additionally, the cross-sectional area of the spine will be calculated. In order to remove the boundary and identify the tumor-affected area, the modified image will then be converted to a binary image. Finally, MATLAB software is used to determine the tumor's volume.

Hasan and Ahmad (2018) created an approach using trilateral filters as preprocessing methods before applying a median filter. For watershed segmentation, this preprocessed image is used. The authors propose that by reducing the detailed texture of the image through smoothing, techniques of pre-processing can be utilized to get around the drawback of over segmentation by the watershed algorithm. Additionally, these methods can help with contrast enhancement, image sharpening using a gaussian high pass filter and noise removal using a median filter.

Lu et al. (2019) uses morphological filtering as a pre-processing method before watershed segmentation. However, this method produces erroneous edge positions as a result of the pre-processing approaches' weak noise filtering.

Sivakumar and Janakiraman (2020) suggest employing edge detection with Enhanced Canny Edge Detection (ECED) to increase the segmentation process' accuracy. Additionally, as a precondition to the Enhanced Canny Edge Detector, they also use a high pass filter. In an effort to increase the sensitivity and accuracy, they employ modified watershed segmentation.

Khan et al. (2019) performs a gamma contrast stretching using a Gaussian filter. Watershed segmentation, followed by post procedures like the

Maximally Stable Extremal Region (MSER) and Histogram Oriented Gradients (HOG), is used to extract features from images of tumors and remove any extraneous characteristics that may have been present after watershed segmentation. For feature selection, chi-square distance is calculated.

Jemima and Vetharaj (2018) concentrate on Dynamic Angle Projection Pattern (DAPP) as a post-processing technique following watershed segmentation. This technique makes use of a 5x5 mask with the centre pixel value rotated 45° in relation to the surrounding pixels. The watershed segmentation image and this masked image are combined, and the pixel intensity is binarized. The intensity can now be read in terms of texture thanks to the decimal encoding of the values. The pooling layer and the convolution layer are the two layers used by the convolutional neural network (CNN) towards the end to classify tumors.

Oo and Khaing (2014) achieve an effective technique by balancing pre-processing and postprocessing. They begin by completing a noise-removal filtering and skull-stripping procedure to make it simpler to identify the tumor location. Watershed segmentation comes next, and morphological erosion is used as a post-processing technique. By removing the tumor's surrounding tissue, this technique highlights the desired area of the brain. Additionally, it shows the spot where the tumor was found.

Bahadure et al., 2017 initially converts an image into its grey-scale equivalent. The noise is subsequently reduced by a median filter to improve the quality of the image. Watershed segmentation is used after this pre-processing method to pinpoint the tumor's extent and highlight its boundaries. The paper uses morphological processes as part of its post processing to provide a clear output image. A system that can detect brain tumors from MRI scans with high computation speed and low complexity can be created by properly combining pre- and postprocessing methods, the watershed algorithm, and threshold segmentation. To produce standardized findings, the system can be assessed against and contrasted with other methods that use similar statistical parameters, such as SSIM, Normalized Absolute Error (NAE), and PSNR.

Seere and Karibasappa (2020) use a combination of median filter, contrast enhancement, and stationary wavelet mechanism to pre-process the

image. After that, segmentation is carried out in two stages, the first of which groups pixels with similar intensities together using threshold segmentation and the second of which using watershed segmentation. They also suggest the use of Support Vector Machine (SVM), a supervised machine-learning technique, to categorize tumors after segmentation.

Herzog, Nitsa J., et al (2021) indicates an implementation of a data processing pipeline on commodity hardware. For the investigation of structural changes and machine learning classification of the condition, it leverages elements of brain asymmetry that were identified from MRI data in the Alzheimer's Disease Neuroimaging Initiative (ADNI) database. The experiments distinguish between people with normal cognition (NC) and patients with early-onset or progressing dementia, yielding promising results. Convolutional neural networks and supervised machine learning methods examined achieve accuracy of 92.5% and 75.0% for NC vs. EMCI and 93.0% and 90.5% for NC vs. AD, respectively. The suggested pipeline provides a prospective low-cost option for the diagnosis of dementia and may be helpful for other brain degenerative conditions that are accompanied by alterations in the brain's asymmetries. On a more practical level, the use of image asymmetry and asymmetry features has the potential to help with the design of end-user applications for early detection of cognitive decline and research into the nature of structural changes in the brain that will run on commodity hardware and be used by doctors and other general practitioners. As shown in this paper, these applications can make use of the generalisation capabilities of machine learning models on MRI data that has not yet been seen.

Deep learning has made significant advancements over typical machine learning algorithms in the last several years, taking a leading role in the automation of our daily lives. Modern deep learning architecture and its optimization for medical picture segmentation and classification are covered in Razzak, Muhammad Imran (2018). Many large research institutions are developing deep learning-based solutions that support the use of deep learning to analyse medical images. Looking at machine learning's more positive side, we hope that sooner rather than later, humans will be replaced in the majority of medical applications, notably

diagnosis. There are a number of issues that limit its expansion, so we shouldn't view it as the sole option. The absence of an annotated dataset is one of the major obstacles. Therefore, the question of whether we will be able to collect enough training data without having an impact on the performance of deep learning algorithms can still be answered. Bigger data yields better results, as demonstrated by recent developments in other applications, but how can big data be applied to healthcare? Due to the sensitivity of healthcare data and other difficulties, deep learning-based applications have so far received excellent feedback; nevertheless, we need look into more advanced deep learning techniques that can deal with complicated healthcare data effectively.

Dhiman, Gaurav, et al(2022) suggests typical extraction approach of medical occurrences. The joint extraction of two tumour event attributes in the corresponding amount of pseudo-labeled data. Pseudo-data generation is presented, and data is added. Additionally, this paper is a result of the pseudo-labeled data's randomness. The 10 rounds of the aforementioned experimental procedure are carried out using an algorithm based on the worldwide random replacement of essential information, which enhances the model's ability to learn from migration. In these 10 iterations, the approach presented in this study came in third as the calculated F1 value. As can be observed, the strategy used in these records yields the F1 value of 74.68 when 1,000 pseudo-the clinical medical event extraction and evaluation task of CCKS2020 electronic medical labelled data are added to the train. Numerous tests on the CCKS2019 and CCKS2020 datasets reveal that this paper's method performs significantly better than the CCMNN extraction and assessment task, surpassing the F1 value (73.52) of the method in the CCKS2020 medical event. Additionally, we might draw the conclusion that, especially for primary tumors, the amount of approach. Additionally, the performance of the approach has significantly improved, the research goal of this study has been accomplished, and the performance of size extraction has increased with the inclusion of pseudo-labeled data to the training set. This paper builds up, peaks, and then decelerates. However, the falsely labelled data to some extent, the model is harmed by the huge amount of randomness in the pseudo- data-generation process suggested by the method in this article because the generated pseudo-data may not always follow the

natural semantics. In order to enhance the quality of pseudo-data generation and further boost the performance of the model, we will now examine pseudo-data-generating methods based on semantic similarity replacement.

The best method for early breast cancer detection is mammography. This device also makes it possible to identify additional diseases and may reveal details about the type of cancer, such as whether it is benign, malignant, or normal. Jasti, V., et al (2022) covers a machine learning and image processing- based evolutionary method for classifying and identifying breast cancer. To assist in the classification and detection of skin diseases, this model integrates image preprocessing, feature extraction, feature selection, and machine learning approaches. The geometric mean filter is applied to improve the quality of the image. Features are extracted using AlexNet. The relief algorithm is used to pick features. The model uses machine learning methods such as least square support vector machine, KNN, random forest, and Nave Bayes for disease categorization and detection. Data gathering from MIAS is utilised in the experimental inquiry. Using image analysis to correctly diagnose breast cancer disease is a benefit of the suggested method.

Based on the enormous success of deep learning technology in the field of computer vision and the issue of numerous unknown objects in the unstructured working environment of service robots, Ding, Yuhan, et al(2022) performs an extensive investigation on the application of deep learning to robot machine vision difficulties. A collection of straightforward and effective visual processing algorithms is also designed in this study in consideration of the algorithm's actual viability. In addition, this study rationally chooses the image capture camera, neural network training platform, and embedded deployment platform in accordance with the unique algorithms of each stage in the vision algorithm scheme and provides a thorough justification for each choice. Additionally, this study constructs a vision system based on a high- resolution colour camera and TOF depth camera and examines the deployment strategy of each algorithm on the embedded platform. The projection relation- ship of the depth map acquired by the TOF camera to the pixel coordinate system of the high-resolution colour camera is established by modelling the coordinate transformation relationship of the same object in

the camera coordinate systems of two cameras. The performance of the model system created in this study is finally examined through experimental analysis in this paper. The results of the experimental research show that the robot machine vision system developed in this paper has a particular impact.

### 3. Proposed methodology

The goal of pre-processing techniques is to improve the image by removing noise, changing contrast, smoothing, eroding, and dilating the image. The detected region impacted by dementia is further enhanced and highlighted using post-processing techniques like k-means clustering and Maximally Stable Extremal Regions (MSER), making it simple to read and comprehend (Figure 1). We can also figure out the type of dementia by number of MSER regions. Table 1 classifies the stage of dementia according to the number of ellipses of MSER .

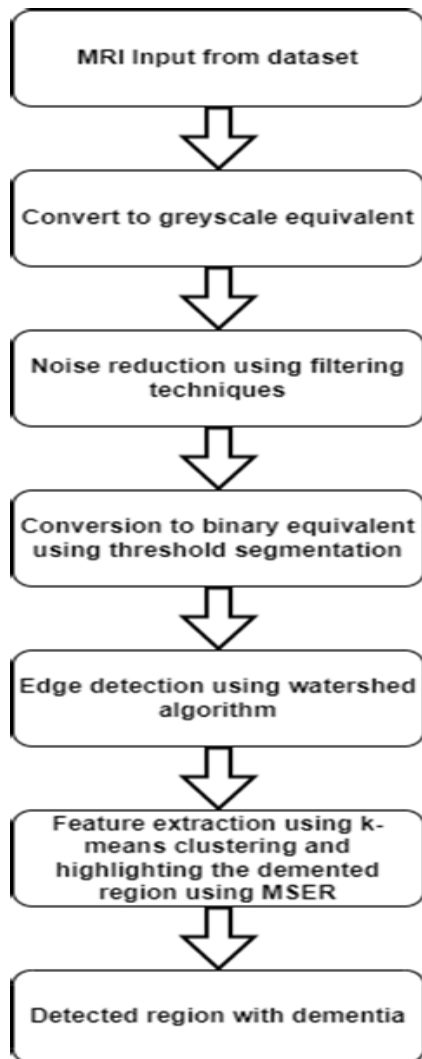


Fig. 1. Methodology proposed

### 3.1 Pre-processing stage

The input is taken from the MRI scan. To make the subsequent processing easier, the main target of this stage is to reduce the amount of disruption and noise in the image (Figure 2)

- Grey-scale conversion: The image's color-scheme is verified, and if it is in another color-scheme, it is transformed to greyscale (Figure 3(A)).
- Median filter: A median filter, which filters nine pixels at a time and fixes the median value of all nine as the output intensity, is used to filter the noise (Figure 3(B)).
- Image smoothening: A  $2 \times 7$  smoothening matrix with a whole row of 1s and 0s is then used to smooth the image. As the smoothening filter moves window by window to average out pixel values, this matrix serves as its operational window. Since values are entered as sums of products, the 1s are utilized to enter pixel values into the matrix without altering them. The 0s provide the matrix a zero-padded input, making it compatible with the ensuing smoothening algorithm (Figure 3(C)).
- Top-hat filter: Noise in the image's foreground is eliminated with the top hat filter. It accomplishes this by removing details and minute components from the image (Figure 3(D)).
- Contrast enhancement: Saturating the top and bottom 1% of the intensity values improves contrast (Sara et al., 2019) (Figure 4(A)).

• Image binarization: By doing this, the complete image is transformed into a matrix of 0s and 1s based on the intensity value. A black and white image is the result of this process (Figure 4(B)).

• Morphological operations: To fill in any holes and gaps inside the borders of various zones, morphological dilation adds pixels, while morphological erosion removes any extra pixels (Figure 4(C)).

### 3.2 Processing stage

After morphological operations, the image is subjected to the following processing techniques.

- Thresholding: A threshold value is established in this on the basis of the average of all intensity values. One is set for pixel intensities over the threshold value, and zero is set for intensities less than the threshold value. Figure 5(A) shows the image after thresholding.



- **Complementing:** The image obtained after threshold algorithm is complemented before being used for watershed segmentation. Complementing the image involves conversion of 0s in the threshold matrix to 1s and vice versa. Figure 5(B) shows the image after complementing
- **Watershed segmentation:** When segmenting an image using watershed segmentation, the entire image matrix is seen as the watershed area, with the image region serving as the catchment basin and the edges of image objects serving as the ridgelines. The higher a pixel is in the catchment area, the brighter it is. The pixel intensities are categorized in accordance with the local maximas acquired from watershed segmentation, which are region-based (Sara et al., 2019). The image following watershed segmentation is shown in Figure 5(C).



**Fig. 2.** Pre-processing Methods.

### 3.3 Post-processing stage

After segmentation, post-processing methods are applied to the image. Maximally Stable Extremal Regions and K-means clustering are the two post-

processing methods employed in the methodology proposed (MSER). Figure 6 shows the order of processing and post-processing techniques.

**K-mean clustering:** The image is divided into 'k' distinct clusters in k-mean clustering. The value of k is assumed to be four for this operation. The clustering is carried out using the least number of pixels from the centroid, with "K" centroids being set. Each of these centroids is processed separately, creating four layers of the image with various pixel groupings. The complete image is made up of these four layers when they are combined. We obtain a segmented MRI for the k-means algorithm based on the region intensity. The clusters that develop precisely segment the MRI into various regions. In general, the quality of segmentation improves as k is increased, but a high value of k creates enormous clusters that make it challenging to distinguish between distinct regions. Therefore, the best value for k was chosen based on the kind of results that were required, which varied depending on the images that were taken. Since k represents the number of segments in the image, choosing a lower value for k will provide segmented MRI with smaller intensities. The image after K-means clustering is shown in Figure 7.

- **Maximally stable extremal regions (MSER):** By combining the identical intensity pixels according to intensity bands, the MSER function fine-tunes the image. This technique links regions of comparable intensity and is used for blob detection.

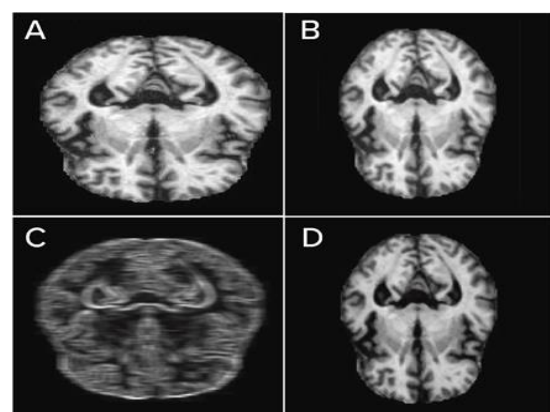


**Fig. 3.** Greyscale image(A), image following median filter (B), image following smoothing(C), and image following top hat filtering(D).

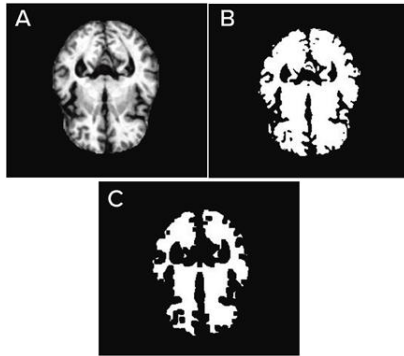


**Fig. 4.** Image following contrast improvement(A), Image following binarization(B) and image following morphological erosion(C).

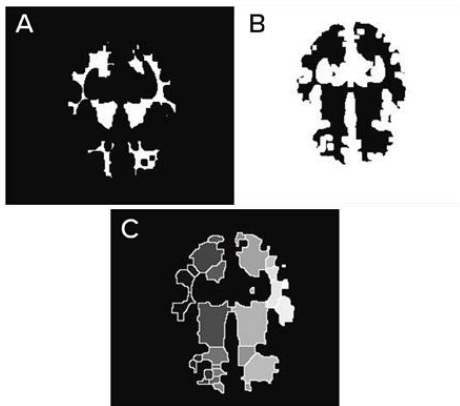


**Fig. 5.** Image following thresholding(A), image following complement(B) and image following watershed segmentation(C)

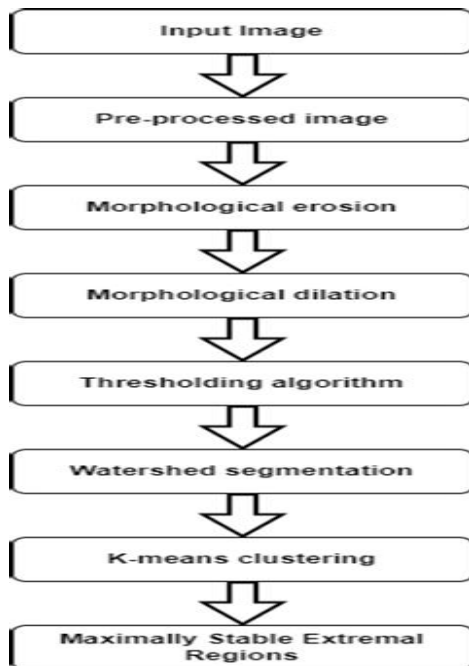


**Fig. 6.** Processing and post-Processing Techniques

#### 4. Experimental outcome

Figure 8(B and C) shows the results of the suggested approach. Figure 8(A) represents the input image and figure 8(B) is the processed image in which the region with dementia is highlighted. Figure 8(C) shows the number of MSER regions. We can refer to table 1 and classify the stage of dementia.

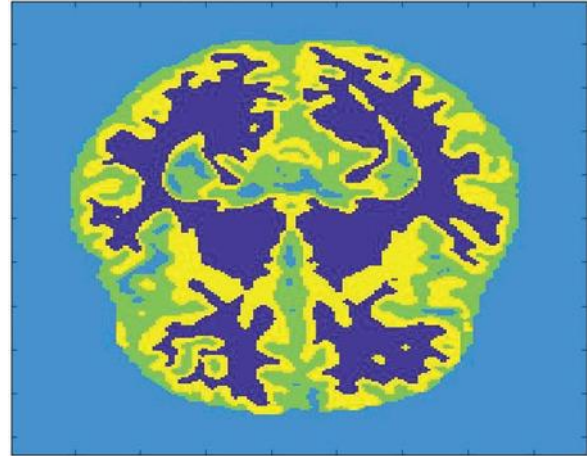


**Fig. 7.** K-Means clustering resulted in an image with four contrasting coloured groups superimposed

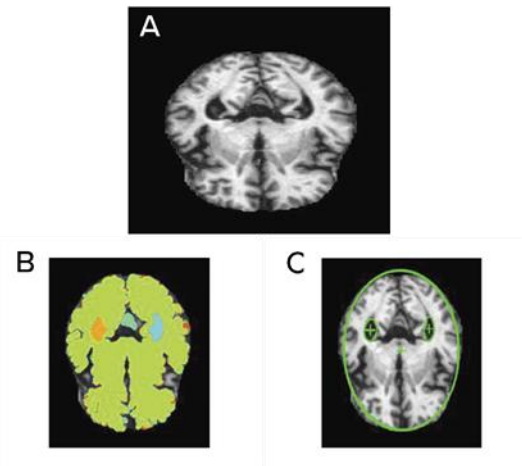


**Fig. 8.** Input image(A), image with MSER(B), image with MSER ellipses and centroid(C).

##### 4.1 Performance Evaluation Metrics

Six measures, Peak Signal-to-Noise Ratio (PSNR), Structural Similarity Index Measure (SSIM), Entropy Feature Similarity Index Measure (FSIM), Normal- ize Cross Correlation (NCC), Normalized Absolute Error (NAE) were used to evaluate a set of images.

- PSNR: It is the ratio of the signal's power to noise's power to distort the signal.

$$PSNR = 10 \log_{10} \left[ \frac{R^2}{MSE} \right]$$

where, 'MSE' is the mean square error and 'R' is maximum fluctuation in input image. The amount of noise creating distortion decreases as PSNR increases. It makes advantage of the MSE between the input and reference images as well as the image datatype range.

- SSIM: It is a normalized measure that is employed to determine how comparable the input and processed images are. Structure, contrast, and luminance serve as comparison criteria.

$$SSIM = \frac{(2\mu_x\mu_y + C_2)(2\sigma_{xy} + C_2)}{(\mu_x^2 + \mu_y^2 + C_1)(\sigma_x^2 + \sigma_y^2 + C_2)}$$

where, ' $\sigma$ ' is the contrast, ' $\mu$ ' is the luminance, and C1, C2 are the constants for stability. SSIM measures the amount of image degradation brought on by preprocessing. The function groups pixels in the processed reference image that have comparable pixel densities.

- FSIM: It is identical to SSIM except that the minor characteristics are contrasted and phase congruency and gradient magnitude are used as comparison criteria.

$$S_L(x) = [S_{PC}(x)]^\alpha [S_G(x)]^\beta$$

where  $\alpha$  and  $\beta$  are parameters used to adjust the relative importance of PC and GM features while ' $S_{PC}$ ' and ' $S_G$ ' are the similarities based on phase congruency (PC) and gradient magnitude (GM). Image quality is assessed using FSIM. Based on changes in light intensity and change in intensity in a specific direction, features of the two images are compared.

- Entropy: It is the measurement of the information a given image carries. Information and entropy are directly proportional.

$$H(X) = -\sum_{i=1}^n p(x_i) \log_b p(x_i)$$

where X denotes the image to be quantified, p(x<sub>i</sub>) denotes probability of level i, b denotes units (as image pixel is coded in bits, b = 2), x<sub>i</sub> denotes level i, and n denotes the number of levels. Entropy measures the texture of the image and so reveals how much information it contains. It converts the pixel intensity value into a width-based numerical parameter.

- NAE: It measures the variation between the original and the processed image. It indicates the difference in numbers between the two photos.

$$NAE = \frac{\sum_{i=1}^m \sum_{j=1}^n (|A_{ij} - B_{ij}|)}{\sum_{i=1}^m \sum_{j=1}^n (A_{ij})}$$

where, for a given size of m x n, A and B are the respective image pixel values of the reference picture and processed image. The precise difference between the processed and reference images is measured by NAE.

- NCC: For template matching, the parameter known as Normalized Cross Correlation (NCC) is used. It is used to look for instances of the original image in the modified image.

$$NCC = \frac{\sum_{i=1}^m \sum_{j=1}^n (|A_{ij} \times B_{ij}|)}{A_{ij}^2}$$

where m x n is the dimension and A and B are, respectively, the reference image and processed image pixel values. NCC measures the similarity between two images. Calculating cross correlation values involves going window by window through the reference and processed images.

## 4.2 Stages of dementia

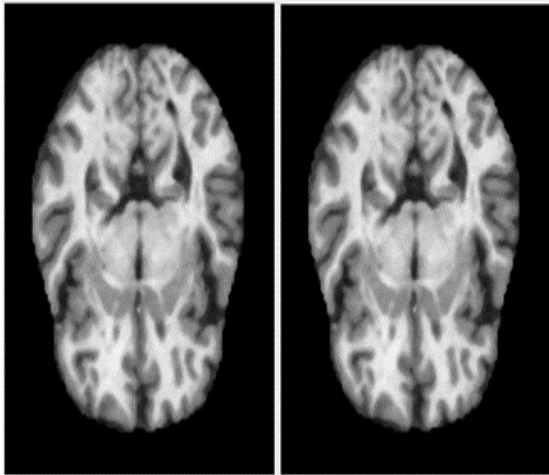
The stage of dementia can be found by counting MSER. The range from a set of 80 images obtained from an opensource image dataset is given in Table 1.

**Table 1.** MSER Count For Stage of Dementia

Stage	MSER count
Non demented	0-1
Very mild	2-5
Mild	6-18
Moderate	19-35

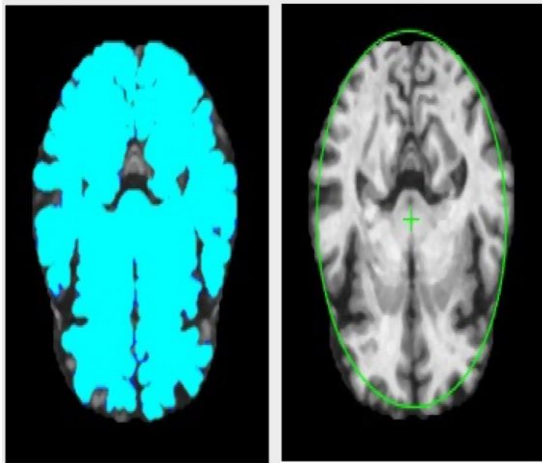
### 4.2.1 Non demented

Figure 9 shows a MSER image and a image with MSER ellipses and centroids of a non demented brain.



**Fig. 9.** Image with MSER(left), Image with MSER ellipses and centroid(right)

#### 4.2.2 Very mildly demented



**Fig. 10.** Image with MSER(left), Image with MSER ellipses and centroid(right)

#### 4.2.3 Mildly demented

ellipses and centroids of a mildly demented brain.

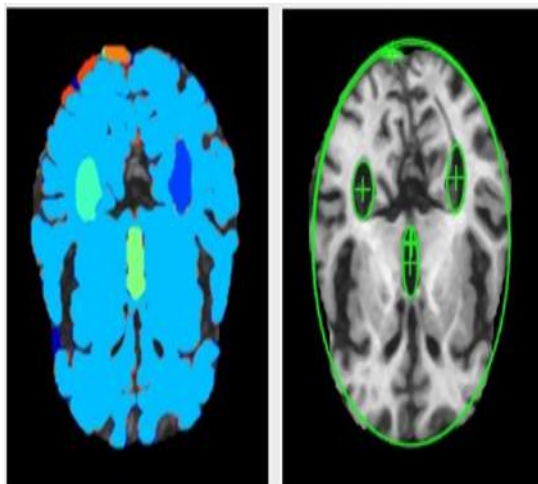


**Fig. 11.** Image with MSER(left), Image with MSER ellipses and centroid(right)

#### 4.2.4 Moderately demented

Figure 12 shows a MSER image and a image with MSER ellipses and centroids of a moderately demented brain.

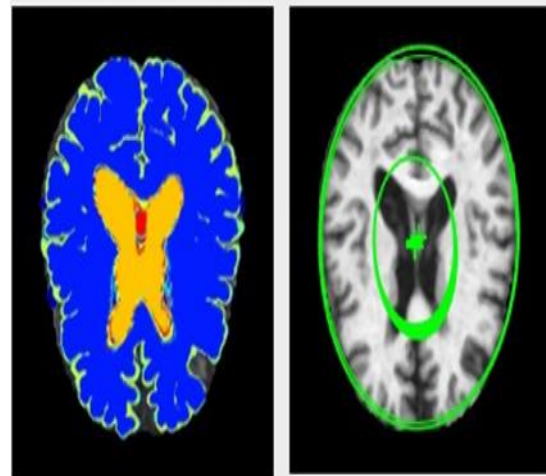


**Fig. 12.** Image with MSER(left), Image with MSER ellipses and centroid(right)

### 5. Discussion

The evaluation parameters for a dataset of selected images were determined. After that, the stage of dementia is found out using MSER. A small subset of the data obtained for evaluation parameters is presented in Table 2 and stage of dementia is presented in table 1. As can be seen from Table 2, the PSNR values obtained are high (up to 29.526, Image 15) and indicate that the signal's strength is substantially greater than the noise's ability to distort it(as it is greater than 1). For SSIM, the closer a value is to 1, the more similar the structure is. The values obtained from the table are more similar to 1 (the highest value being 0.961530 for Image 15), suggesting that the processed image has retained its structural identity. The closer a value is to 1 when FSIM values are normalised, the better the outcome. The highest result here is 0.972035 for Image 11. Entropy values range from 4-5, and those found in the table are closer to the highest values, which can reach up to 4.778 for Image 12. When it comes to NAE, the lower the value, the higher the image quality. The table's observations demonstrate that the image quality is good because NAE values are closer to 0, with Image 15's minimum value being 0.064. The table illustrates that for NCC, the closer a value is to 1, the better the match. The best outcome was 0.996827 for Image 15. MSER are found and the MSER ellipses are counted for various images.

The results are grouped together to classify the stage of dementia (table 1).

Image	PSNR	SSIM	FSIM	ENTROPY	NAE	NCC
1	27.371524	0.946219	0.967957	4.746582	0.09588	0.995101
2	26.256491	0.936248	0.963464	4.750389	0.113148	0.993804
3	26.968077	0.934532	0.970604	4.734493	0.101682	0.993927
4	26.949595	0.949845	0.968642	4.7629	0.098837	0.994676
5	17.151059	0.90396	0.93241	4.547644	0.41492	0.992589
6	26.391163	0.943152	0.966561	4.739446	0.11637	0.993567
7	27.76375	0.953313	0.968791	4.720305	0.084461	0.995692
8	26.372002	0.936971	0.966059	4.693974	0.114837	0.992847
9	28.493194	0.95599	0.970761	4.721485	0.075915	0.996057
10	26.418831	0.942812	0.966091	4.671225	0.114594	0.993545
11	28.469036	0.958441	0.972035	4.714509	0.075059	0.996619
12	28.652408	0.95251	0.968091	4.77823	0.070864	0.995563
13	25.957702	0.931023	0.962301	4.751259	0.127515	0.99258
14	23.997298	0.942436	0.962388	4.72949	0.151965	0.994664
15	29.526992	0.96153	0.970849	4.745753	0.064073	0.996827

**Table 2.** Statistical Analysis

## 6. Comparative analysis

Two already-existing algorithms are contrasted with the one that is being suggested. These algorithms differ primarily in the pre- and post-processing methods they use in conjunction with watershed segmentation and thresholding. The same collection of images that were processed for performance assessment is used for this study. The pre-processes suggested by Tarhini and Shbib (2020) involve the input MRI scan being converted from RGB to greyscale, the use of a median filter and a Gaussian averaging filter to reduce noise, and the application of a Gaussian high pass filter to sharpen and enhance the image. Segmentation using the watershed

algorithm comes next. The last step involves morphological techniques. While Oo and Khaing (2014) also utilize watershed segmentation and morphological operation for image transformation, they simply apply the average filter as part of the pre-processing stage to smooth out the image. With the aid of the evaluation parameters, the output images are measured and show a clear change as a result of these alterations in the pre-processing and post-processing stages.

As can be observed in Table 3, the PSNR value of the algorithm proposed is 26.44927, which is noticeably high when compared to the values of the other two algorithms, suggesting that the algorithm maintains the image quality. The suggested algorithm's FSIM and SSIM values are 0.965134 and 0.943265, respectively, and they significantly outperform those of Oo and Khaing (2014) and Tarhini and Shbib (2020). This demonstrates the higher processing capabilities of the suggested method. The suggested algorithm has an entropy value of 4.720512, which is noticeably high when compared to those of Oo and Khaing (2014) and Tarhini and Shbib (2020), as can be seen from the table presented. These numbers show that, when compared to images processed using the other methods under consideration, the image processed using the proposed approach preserves the most information. The lowest NAE value found was 0.121341; this is a lower number than those of the other two procedures.

The NCC value in Oo and Khaing (2014) was 0.399596, whereas the value in Tarhini and Reda (2020) was 0.440804, indicating a high level of distortion in the output image relative to the input. The proposed algorithm's NCC value is noticeably greater, which denotes higher correlation. The evaluation parameters of the suggested algorithm appear to be more precise and acceptable when compared to Oo and Khaing (2014) and Tarhini and Shbib (2020). The suggested algorithm has the greatest values for SSIM and FSIM, the two parameters that are most crucial for assessing the quality of processing. This indicates that the image has been thoroughly processed while keeping its originality, giving it a competitive edge over the other two algorithms.

**Table 3.** Comparative analysis

Parameters	Proposed algorithm	Tarhini, G. M. and Shbib, R. 2020	Oo, S. Z. and Khaing, A. 2014
PSNR	26.44927	8.804921	7.548608
SSIM	0.943265	0.064541	0.164087
FSIM	0.965134	0.358433	0.51399
Entropy	4.720512	3.937836	3.115536
NAE	0.121341	1.056724	1.027723
NCC	0.994537	0.399596	0.440804

### 7. Conclusion

MRI scans have become more significant in medical research in recent years. The goal of the proposed study is to reliably extract the dementia region from an MRI image using a threshold algorithm and watershed segmentation, and then use MSER to categorize its stage. The process is divided into two parts. The first stage contains pre-processing techniques such the Top-hat filter, median filter, morphological erosion and dilation, which are used to remove undesirable noise from the image. The second stage comprise of thresholding and watershed segmentation, which is used to further process the image. The pre-processed image is divided into segments based on intensity levels of pixels in the second stage using the watershed segmentation and threshold algorithm. Following the calculation of the MSER, the dementia region is effectively emphasized in the resultant image according to its stage. Several MRI scans of the demented brain selected from a dataset are used to test and confirm the accuracy and reproducibility of the entire technique. By computing parameters on the output images, including PSNR, SSIM, and entropy, the system's performance is assessed. These statistical metrics' averages were determined using a wider dataset. The PSNR was calculated to be 26.44927, the SSIM to be 0.943265, the FSIM to be 0.965134, and the average entropy to be 4.720512. It was determined that the normalized absolute error was 0.121341 and the normalized cross correlation was 0.994537. These numbers demonstrate how effective the algorithm is in processing images.

### 8. Future scope

The algorithm's future potential includes using deep learning, machine learning and neural networks to train the dataset. Training lessens the need for human involvement while enhancing the usefulness of dynamic data. By recognizing specific patterns or chains, it also improves results' sensitivity and accuracy. To further improve the outcomes, several combinations of more complex pre- and post-processing algorithms might be applied. Image processing is a highly sought-after instrument for upcoming medical research because of its adaptability and precision. Other fields like remote sensing, image editing and restoration, transmission and encoding, etc. have also benefited from the use of image processing. Computer vision is one of the most fascinating and practical uses of image processing. To enable a computer to view, recognise objects, and interpret the entire environment, computer vision is utilised. Self-driving cars, drones, and other devices are major applications for computer vision. Obstacle detection, path recognition, and environmental comprehension are all made easier by CV.

### Conflicts of Interest

The authors declare no conflicts of interest.

### References

- [1] Abdallah et al., 2019 "Research in medical imaging using image processing techniques." Medical Imaging-Principles and Applications (2019).
- [2] Anitha and Jyothi, 2016. A segmentation technique to detect the Alzheimer's disease using image processing. In 2016 International Conference on Electrical, Electronics, and Optimization Techniques (ICEEOT) (pp. 3800-3801). IEEE.
- [3] Bahadure, et al., 2017. Image analysis for MRI based brain tumor detection and feature extraction using biologically inspired BWT and SVM. International journal of biomedical imaging, 2017.
- [4] Cui et al., 2009. Malignant lesion segmentation in contrast-enhanced breast MR images based on the marker-controlled watershed. Medical physics, 36(10), 4359-4369.
- [5] Dhage et al., 2015. Watershed segmentation brain tumor detection. In 2015 International Conference on Pervasive Computing (ICPC) (pp. 1-5). IEEE.

- [6] Dhankhar et al., 2010. Brain MRI Segmentation using K-means Algorithm. 10.13140/RG.2.1.4979.0567.
- [7] Dhiman et al.,2022. "A novel machine-learning-based hybrid CNN model for tumor identification in medical image processing." Sustainability 14.3 (2022): 1447.
- [8] Ding et al.,2022. "Research on computer vision enhancement in intelligent robot based on machine learning and deep learning." Neural Computing and Applications 34.4 (2022): 2623-2635.
- [9] Hagler Jr et al.,2019. "Image processing and analysis methods for the Adolescent Brain Cognitive Development Study." Neuroimage 202 (2019): 116091.
- [10] Hasan et al., 2018. Two-step verification of brain tumor segmentation using watershed-matching algorithm. Brain informatics, 5(2), 1-11.
- [11]Herzog et al., 2021. "Brain asymmetry detection and machine learning classification for diagnosis of early dementia." Sensors 21.3 (2021): 778.
- [12]Hore and Ziou, 2010. Image quality metrics: PSNR vs. SSIM. In 2010 20th international conference on pattern recognition (pp. 2366-2369). IEEE.
- [13]Hou et al.,2021. "The state-of-the-art review on applications of intrusive sensing, image processing techniques, and machine learning methods in pavement monitoring and analysis." Engineering 7.6 (2021): 845-856.
- [14]Jasti et al.,2022. "Computational technique based on machine learning and image processing for medical image analysis of breast cancer diagnosis." Security and Communication Networks 2022 (2022).
- [15]Jemimma et al., 2018. Watershed algorithm based DAPP features for brain tumor segmentation and classification. In 2018 International Conference on Smart Systems and Inventive Technology (ICSSIT) (pp. 155-158). IEEE.
- [16]Khan et al., 2019. Brain tumor detection and classification: A framework of marker-based watershed algorithm and multilevel priority features selection. Microscopy research and technique, 82(6), 909-922.
- [17] Liu, Xiaolong et al.,2019. "Recent progress in semantic image segmentation." Artificial Intelligence Review 52.2 (2019): 1089-1106.
- [18]Lu et al., 2019. An improved watershed segmentation algorithm of medical tumor image. In IOP conference series: materials science and engineering (Vol. 677, No. 4, p. 042028). IOP Publishing.
- [19]Mason et al., 2019. Comparison of objective image quality metrics to expert radiologists' scoring of diagnostic quality of MR images. IEEE transactions on medical imaging, 39(4), 1064-1072.
- [20]Mahmud et al., 2020. Biomedical Image Processing: Spine Tumor Detection from MRI image using MATLAB. The Journal of Contents Computing, 2(2), 225-235.
- [21]Marias, Kostas 2021. "The Constantly Evolving Role of Medical Image Processing in Oncology: From Traditional Medical Image Processing to Imaging Biomarkers and Radiomics." Journal of imaging 7.8 (2021): 124.
- [22]Mishra et al., 2021. Performance evaluation of brain tumor detection using watershed Segmentation and thresholding. International Journal on Smart Sensing and Intelligent Systems, 14(1), 1-12.
- [23]Mohtasham Khani et al.,2020. "Deep-learning-based crack detection with applications for the structural health monitoring of gas turbines." Structural Health Monitoring 19.5 (2020): 1440-1452.
- [24]Mustaqeem et al., 2012. An efficient brain tumor detection algorithm using watershed thresholding based segmentation. International Journal of Image, Graphics and Signal Processing, 4(10), 34.
- [25]Ngugi et al., 2021. "Recent advances in image processing techniques for automated leaf pest and disease recognition—A review." Information processing in agriculture 8.1 (2021): 27-51.
- [26]Oo et al., 2014. Brain tumor detection and segmentation using watershed segmentation and morphological operation. International Journal of Research in Engineering and Technology, 3(3), 367-374.
- [27]Pambrun et al., 2015. Limitations of the SSIM quality metric in the context of diagnostic imaging. In 2015 IEEE International Conference on Image Processing (ICIP) (pp. 2960-2963). IEEE.
- [28]Patro et al., 2019. Early detection of Alzheimer's disease using image processing. Int. J. Eng. Res. Technol.(IJERT), 8(05).
- [29]Razzak et al.,2018. "Deep learning for medical

- image processing: Overview, challenges and the future.” *Classification in BioApps* (2018): 323-350.
- [30] Salvi et al., 2021. ”The impact of pre-and post-image processing techniques on deep learning frameworks: A comprehensive review for digital pathology image analysis.” *Computers in Biology and Medicine* 128 (2021): 104129.
- [31] Sara et al., 2019. Image quality assessment through FSIM, SSIM, MSE and PSNR—a comparative study. *Journal of Computer and Communications*, 7(3), 8-18.
- [32] Shahin and Osama, 2018. Brain tumor detection using watershed trans- form. *Annals of Clinical and Cytology and Pathology*, 4, 1-6.
- [33] Seere et al., 2020. Threshold segmentation and watershed segmentation algorithm for brain tumor detection using support vector machine. *European Journal of Engineering and Technology Research*, 5(4), 516-519.
- [34] Sivakumar and Janakiraman, 2020. A novel method for segmenting brain tumor using modified watershed algorithm in MRI image with FPGA. *Biosystems*, 198, 104226.
- [35] Słuzek and Andrzej, 2016. Improving performances of MSER features in matching and retrieval tasks. In *European Conference on Computer Vision* (pp. 759-770). Springer, Cham.
- [36] Sreedhar et al., 2020. ”A comparative study of melanoma skin cancer detection in traditional and current image processing techniques.” 2020 Fourth International Conference on I-SMAC (IoT in Social, Mobile, Analytics and Cloud)(I-SMAC). IEEE, 2020.
- [37] Tarhini et al., 2020. Detection of brain tumor in mri images using watershed and threshold-based segmentation. *International Journal of Signal Processing Systems*, 8(1), 19-25.
- [38] Wang et al., 2019. ”A review on weed detection using ground-based machine vision and image processing techniques.” *Computers and electronics in agriculture* 158 (2019): 226-240.
- [39] Zhao et al., 2006. Image matching by normalized cross-correlation. In 2006 IEEE international conference on acoustics speech and signal processing proceedings (Vol. 2, pp. II-II). IEEE.
- [40] Zhang et al., 2011. FSIM: A feature similarity index for image quality assessment. *IEEE transactions on Image Processing*, 20(8), 2378-2386.
- [41] Zaman et al., 2017. *Advances in Visual Informatics: 5th International Visual Informatics Conference, IVIC 2017, Bangi, Malaysia, November 28–30, 2017, Proceedings* (Vol. 10645). Springer.